# Implicit local radial basis function method for solving two-dimensional time fractional diffusion equations

Wei, Song; Chen, Wen; Hon, Yiu-Chung

**Published in:**
Thermal Science

**Published: 01/01/2015**

**Document Version:**
Final Published version, also known as Publisher's PDF, Publisher's Final version or Version of Record



**Published version (DOI):**
10.2298/TSCI15S1S59W

**Publication details:**
Wei, S., Chen, W., & Hon, Y.-C. (2015). Implicit local radial basis function method for solving two-dimensional time fractional diffusion equations. *Thermal Science*, *19*, 59-67. https://doi.org/10.2298/TSCI15S1S59W

# IMPLICIT LOCAL RADIAL BASIS FUNCTION METHOD FOR SOLVING TWO-DIMENSIONAL TIME FRACTIONAL DIFFUSION EQUATIONS

by

***Song WEI[a], Wen CHEN[a]*, and Yiu-Chung HON[b]****

[a] State Key Laboratory of Hydrology – Water Resources and Hydraulic Engineering, College of Mechanics and Materials, Hohai University, Nanjing , China
[b] Department of Mathematics, City University of Hong Kong, Hong Kong, China

Original scientific paper
DOI: 10.2298/TSCI15S1S59W

*Based on the recently developed local radial basis function method, we devise an implicit local radial basis function scheme, which is intrinsic mesh-free, for solving time fractional diffusion equations. In this paper the L1 scheme and the local radial basis function method are applied for temporal and spatial discretization, respectively, in which the time-marching iteration is performed implicitly. The robustness and accuracy of this proposed implicit local radial basis function method are demonstrated by the numerical example. Furthermore, the sensitivities of the shape parameter c and the number of nodes in the local sub-domain to the accuracy of numerical solutions are also investigated.*

Key words: *local radial basis function, time fractional diffusion equation, implicit scheme*

## Introduction

Time fractional diffusion models are recently becoming popular for characterizing anomalous diffusion and complex phenomena. Anomalous diffusion phenomena have been widely observed in various scientific and engineering fields, such as heat conduction [1, 2], solute transport [3, 4], dissipation [5], system control [6], chaos [7], transport in fractal objects [8, 9], *etc*. These complex phenomena possess the properties of history dependence, heavy tailedness or long-range correlation [10]. From theoretical and experimental studies, fractional derivative has been considered as a suitable tool to characterize these properties. As a consequence, fractional derivative have been widely introduced in various models to capture some anomalous phenomena with considerable success [11-14].

Due to the introduction of the fractional derivative, it is challenging to obtain the analytical solutions of fractional differential equations, particularly for problems with complex initial and boundary conditions. Various numerical methods have been proposed to solve fractional differential equations in which the finite difference method (FDM) is presently the dominant method for solving these fractional diffusion problems [15-18]. However, the FDM encounters inconvenience when applied to problems with curved boundaries.

In the last decades, collocation methods based on radial basis functions (RBF) have gradually attracted the attention of many researchers for solving partial differential equations

* Corresponding authors; e-mail: chenwen@hhu.edu.cn; benny.hon@cityu.edu.hk

[19-23]. These RBF-based collocation methods belong to the family of mesh-free methods which require only scattered nodes in the problem domain and boundary. The avoidance of constructing grids enables these mesh free methods advantage in tackling high-dimensional problems with irregular domains. The RBF methods approximate the solutions by a linear combination of the RBF, which are globally defined, and hence the resultant interpolation matrices are fully dense and highly ill-conditioned. In addition, some RBF contain a free shape parameter whose chosen value is critical to the accuracy of the numerical results [24, 25]. The search for optimal shape parameter has been an open problem and recently some theoretical and numerical works have been made [26-28]. On the other hand, the global RBF method is hindered for large scale problems. To mitigate the aforementioned demerits, the local radial basis function (LRBF) method has been proposed. Instead of using all the nodes in the domain and on the boundary, the LRBF method only uses data in the neighboring nodes which fall in the influence domain. As a result, the resultant matrix of LRBF is sparse and hence is feasible for solving larger scale problems [29, 30]. The LRBF method has recently been employed to some complex problems such as thermo-driven fluid-flow [31], Navier-Stocks equations [32], phase-change phenomena [33], *etc*. More details can be found from [29, 31, 34-37].

In this paper authors focus on the investigation of solving time fractional diffusion equations by employing implicit local basis radial function method. The L1 approximation scheme is employed for temporal discretization, and the local RBF method is applied for spatial discretization. The influences of $c$ (the shape parameter), $ns$ (the total number of nodes fallen within the local sub-domain), $dt$ (temporal step) and $h$ (grid distance) on the accuracy of numerical results are also investigated.

## Governing equation and discretization

### *Time fractional diffusion equation*

The considered time fractional diffusion equation is stated as:

$$ {}^{C}D_t^{\alpha} u(\mathbf{x},t) + \lambda u(\mathbf{x},t) = K\Delta u(\mathbf{x},t) + q(\mathbf{x},t),\ 0 < \alpha(t) < 1,\ \mathbf{x} \in \Omega,\ t > 0 \tag{1} $$

where $K > 0$ is a generalized diffusion coefficient, $\lambda$ – the reaction coefficient, $q(\mathbf{x},t)$ – the source term, and $u(\mathbf{x},t)$ represents mass, concentration, or other physical quantities. ${}^{C}D$ denotes the Caputo definition, and $\alpha \in (0,1)$ is the fractional derivative.

Subject to boundary conditions:

$$ L_{\mathrm{b}} u(\mathbf{x},t) = g(\mathbf{x},t), \quad \mathbf{x} \in \Gamma,\ t > 0 \tag{2} $$

and initial condition:

$$ u(\mathbf{x},0) = f(\mathbf{x}), \quad \mathbf{x} \in \Omega \tag{3} $$

where $L_{\mathrm{b}}$ is the boundary operator, and $f$ and $g$ are given functions.

In this paper, we employ the Caputo definition for calculation, and the definition is stated as:

$$ {}^{C}D_t^{\alpha} f(t) = \frac{1}{\Gamma(1-\alpha)} \int_0^t \frac{f'(\tau)}{(t-\tau)^{\alpha}}\, \mathrm{d}\tau, \quad 0 < \alpha < 1 \tag{4} $$

### *Time fractional derivative discretization*

Based on the L1 approximation scheme [38], eq. (4) can be rewritten as:

$$
\begin{aligned}
{}^{C}D_t^{\alpha}u(x,t_{n+1}) &= \frac{1}{\Gamma(1-\alpha)}\sum_{k=0}^{n}\frac{u(\mathbf{x},t_{k+1})-u(\mathbf{x},t_k)}{dt}\int_{kdt}^{(k+1)dt}\frac{1}{(t_{j+1}-\tau)^{\alpha}}\mathrm{d}\tau \\
&\approx \frac{1}{\Gamma(1-\alpha)}\sum_{k=0}^{n}\frac{u(\mathbf{x},t_{n-k+1})-u(\mathbf{x},t_{n-k})}{dt}\int_{kdt}^{(k+1)dt}\frac{1}{r^{\alpha}}\mathrm{d}\tau \\
&= \begin{cases} \dfrac{dt^{-\alpha}}{\Gamma(2-\alpha)}(u^{n+1}-u^{n})+\dfrac{dt^{-\alpha}}{\Gamma(2-\alpha)}\displaystyle\sum_{k=1}^{n}(u^{n-k+1}-u^{n-k})\left[(k+1)^{1-\alpha}-k^{1-\alpha}\right] & n\geq 1 \\ \dfrac{dt^{-\alpha}}{\Gamma(2-\alpha)}(u^{1}-u^{0}) & n=0 \end{cases} \\
&= \begin{cases} a_0(u^{n+1}-u^{n})+a_0\displaystyle\sum_{k=1}^{n}b_k(u^{n-k+1}-u^{n-k}) & n\geq 1 \\ a_0(u^{1}-u^{0}) & n=0 \end{cases}
\end{aligned} \tag{5}
$$

where $a_0 = dt^{-\alpha}/\Gamma(2-\alpha)$, $b_k = (k+1)^{1-\alpha} - k^{1-\alpha}$, $k$ = 1, 2,..., $n$, $dt$ is the temporal step and $u^k$ – the abbreviation of $u(\mathbf{x}, t_k)$.

For eq. (4) , substituting (5) into (1), we obtain:

$$
\begin{cases} a_0(u^{n+1}-u^{n})+a_0\displaystyle\sum_{k=1}^{n}b_k(u^{n-k+1}-u^{n-k})+\lambda u^{n+1} = K\Delta u^{n+1}+q^{n+1} & n\geq 1 \\ a_0(u^{1}-u^{0})+\lambda u^{1} = K\Delta u^{1}+q^{1} & n=0 \end{cases} \tag{6}
$$

further re-arrangement leads to:

$$
a_0u^{n+1}+\lambda u^{n+1}-K\Delta u^{n+1} = \begin{cases} a_0u^{n}-a_0\displaystyle\sum_{k=1}^{n}b_k(u^{n-k+1}-u^{n-k})+q^{n+1}, & n\geq 1 \\ a_0u^{0}+q^{1}, & n=0 \end{cases} \tag{7}
$$

where $q^{n+1} = q(\mathbf{x}, t_{n+1})$, and $n$ = 0, 1,...,$N$.

For eqs. (1)-(3) and (7), let $L$ represent an operator given by:

$$
L(*) = \begin{cases} (a_0+\lambda-K\Delta)(*), & x\in\Omega \\ L_{\mathrm{b}}(*), & x\in\Gamma \end{cases} \tag{8}
$$

and $\ell^n$ by:

$$
\ell^n = \begin{cases} a_0u^{0}+q_1,\ n=0,\mathbf{x}\in\Omega \\ a_0u^{n}-a_0\displaystyle\sum_{k=1}^{n}b_k(u^{n-k+1}-u^{n-k})+q^{n+1},\ n\geq 1,\mathbf{x}\in\Omega \\ g(x,t_{n+1}),\ \mathbf{x}\in\Gamma \end{cases} \tag{9}
$$

Thus, eqs. (1)-(3) can be rewritten as:

$$
L\ u(\mathbf{x},t_{n+1}) = \ell^n \tag{10}
$$

*Spatial discretization by the LRBF method*

The LRBF method employed for spatial discretization has recently been given by Sarler *et al.* [30, 39, 40]. The idea of LRBF method is to collocate $N$ distinct interpolation points on the problem domain and its boundary and assume that, for each point $\mathbf{x}_k$ ($k$ = 1, 2, ..., $N$), there is an influence domain (sub-domain) $\Omega_k = \{\mathbf{x}_{k_i}\}_{i=1}^{ns}$ ($i$ = 1, 2,...,$ns$), where $ns$ denotes the number of points fallen within the sub-domain. Through the implicit local radial basis function approach, $u(\mathbf{x}_k, t_{n+1})$ in (1) can be approximated by $\hat{u}(\mathbf{x}_k, t_{n+1})$ in the form:

$$u(\mathbf{x}_k, t_{n+1}) \approx \hat{u}(\mathbf{x}_k, t_{n+1}) = \sum_{i=1}^{ns} \lambda_{k_i}^{n+1} \phi\left(\left\|\mathbf{x}_k - \mathbf{x}_{k_i}\right\|\right) \tag{11}$$

where $\{\lambda_{k_i}^{n+1}\}$ are unknown coefficients of the $(n + 1)^{\text{th}}$ time layer and $\phi$ is a radial basis function. In this paper, we employ the commonly used multiquadric (MQ) radial basis function defined as:

$$\phi\left(\left\|\mathbf{x}_i - \mathbf{x}_j\right\|\right) = \sqrt{\left\|\mathbf{x}_i - \mathbf{x}_j\right\|^2 + c^2} \tag{12}$$

where $\left\|\mathbf{x}_i - \mathbf{x}_j\right\|$ denotes the distance between $\mathbf{x}_i$ and $\mathbf{x}_j$, and $c$ is called as shape parameter.

We obtain the matrix form:

$$\hat{\mathbf{u}}_{\Omega_k}^{n+1} = A_k \{\lambda_k\}^{n+1} \tag{13}$$

where $\hat{\mathbf{u}}_{\Omega_k}^{n+1} = [\hat{u}(\mathbf{x}_{k_1}, t_{n+1}),...,\hat{u}(\mathbf{x}_{k_m}, t_{n+1})]^T$, $\{\lambda_k\}^{n+1} = [\lambda_{k_1}^{n+1},...,\lambda_{k_{ns}}^{n+1}]^T$, and $A_k = [\phi(\|x_{k_i} - x_{k_j}\|)]_{1 \le i,j \le ns}$ is an symmetric coefficient matrix.

The coefficient vector $\{\lambda_k\}^{n+1}$ in (13) can be obtained by:

$$\{\lambda_k\}^{n+1} = (A_k)^{-1} \hat{\mathbf{u}}_{\Omega_k}^{n+1} \tag{14}$$

Substituting (11) and (14) into (8), $L\hat{u}(\mathbf{x}_k, t_{n+1})$ can be expressed as:

$$L\hat{u}(\mathbf{x}_k, t_{n+1}) = \sum_{i=1}^{ns} \lambda_{k_i}^{n+1} L\phi\left(\left\|\mathbf{x}_k - \mathbf{x}_{k_i}\right\|\right) = \Psi_k \left(A_k\right)^{-1} \hat{\mathbf{u}}_{\Omega_k}^{n+1} = \Phi_k \hat{\mathbf{u}}_{\Omega_k}^{n+1} \tag{15}$$

where $\Psi_k = [L\phi(\|\mathbf{x}_k - \mathbf{x}_{k_1}\|), ..., L\phi(\|\mathbf{x}_k - \mathbf{x}_{k_{ns}}\|)]$ and $\Phi_k = \Psi_k (A_k)^{-1} = [\Phi_{k_1},...,\Phi_{k_{ns}}]$.

This equation is given in the local form and we can get the global form $\Phi$ from $\Phi_k$ by inserting zeros into the corresponding position. As a result, we obtain the sparse system of equation:

$$\Phi \hat{\mathbf{u}}^{n+1} = \ell^n \tag{16}$$

where $\Phi = [\Phi_1,...,\Phi_N]$, $\hat{\mathbf{u}}^{n+1} = [\hat{u}(x_1, t_{n+1}),...,\hat{u}(x_N, t_{n+1})]^T$, and $N$ denotes the total number of nodes in the whole domain. From eqs. (8)-(10), (15), and (16), the approximate solution $\hat{u}(\mathbf{x}, t)$ can be obtained by solving the above sparse system.

## Numerical results

This section tests the proposed implicit LRBF method for solving time fractional diffusion equations. The collocation points are distributed on the domain $\Omega = \{(x, y) | 0 \le x, y \le 2\}$, and its boundary $\partial\Omega$. The root-mean-square-error is defined by:

$$L_{\text{rms}} = \sqrt{\frac{1}{NM}\sum_{i=1}^{N}\sum_{j=1}^{M}\left|u(x_i, y_j, t) - \hat{u}(x_i, y_j, t)\right|^2}$$

where $u(x_i, y_j, t)$ and $\hat{u}(x_i, y_j, t)$ represent the exact and numerical solutions of the time fractional diffusion equation, respectively. The MQ-RBF $\phi(r) = (r^2 + c^2)^{1/2}$ is employed in this section and the solutions in the time interval $T \in [0, 1]$ are considered in the example in which we let $\alpha = 0.9$.

**Example.** Consider a 2-D time fractional diffusion equation:

$$\frac{\partial^\alpha u(x,y,t)}{\partial t^\alpha} + u(x,y,t) = \Delta u(x,y,t) + Q(x,y,t), \quad 0 \le x, \quad y \le 2, \quad t > 0$$

subject to zero initial condition $u(x, y, 0) = 0,$ and Dirichlet boundary condition:

$$u(x,y,t) = t^2 \sin\frac{\pi x}{2}\sin\frac{\pi y}{2}, \quad x, \quad y \in \partial\Omega$$

The source term:

$$Q(x,y,t) = \left[\frac{2t^{2-\alpha}}{\Gamma(3-\alpha)} + \left(1 + \frac{\pi^2}{2}\right)t^2\right]\sin\frac{\pi x}{2}\sin\frac{\pi y}{2}$$

The exact solution is taken as $u(x,y,t) = t^2 \sin(\pi x/2)\sin(\pi y/2)$.

For various numbers of *ns*, grid distance size *h* and temporal step *dt*, the *c*- $L_{\text{rms}}$ curves are shown in fig. 1. It is observed that when *ns* (*e. g.*, *ns* = 5, 9) is small, with the increase of shape parameter *c*, the accuracy of numerical results improves at beginning until reaching the peak and begins to decline and tends to be stable in a wide range. However, if *ns* becomes large, *i. e.*, 13- and 16-point scheme shown in fig. 1, there may not exist the optimal shape parameter *c*. As shown in fig. 2 and tab.1, the smaller the *ns*, the larger the range of $C_{\text{stable}}$ is obtained. What should be noticed is that the range of $C_{\text{stable}}$ is an approximate range. In some cases, we may even obtain a better result when the selected shape parameter exceeds the $C_{\text{stable}}$, but the results gained by the nearby shape parameter may become unstable.

From fig. 1 and tab. 1, it can be seen that as *dt* decreases, the accuracy of numerical results improves, while the range of $C_{\text{stable}}$ decreases as *dt* gets smaller. This may be partly caused by the memory and hereditary properties of time fractional derivative, namely, the value of $u^{n+1}$ is influenced by the value of $u^k$ ($k$ = 0, 1,...,$n$). Therefore, the smaller the time step, the larger the accumulated error, which results in unstable numerical results.

Figure 3 displays the $L_{\text{rms}}$ error curves of the global MQ. It can be seen that the stable range of *c* is from 0.06 to 0.94 and the $L_{\text{rms}}$ < 5.40E-3. According to tab.1, we know that under the same condition ($N$ = 441, $dt$ = 0.1), the stable range of *c* is from 1.6 to 159 and $L_{\text{rms}}$ < 6.74E-3 by using the local MQ with *ns* = 5. In the stable range, the accuracy of the global method is little higher than that of the local method expect near the optimal *c*. In addition, if the grid distance becomes smaller, such as *h* = 0.05, the results of the global MQ may deteriorate or even incorrect due to the ill-condition problem.

## Conclusions

This paper presents the application of the local RBF method in solving the 2-D time fractional diffusion equations. Unlike the global RBF method, the local RBF method is merely based on the local collocation nodes and the time-marching is performed in an implicit way. It

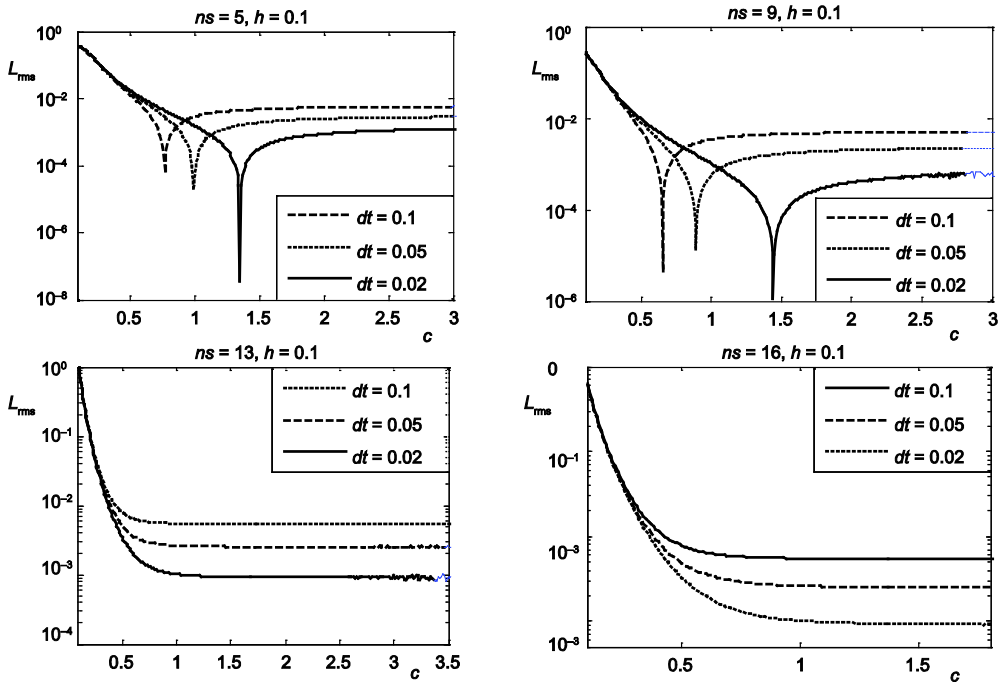


**Figure 1. The evolution curves of $L_{rms}$ with $c$ by using different $ns$ with variable time steps**

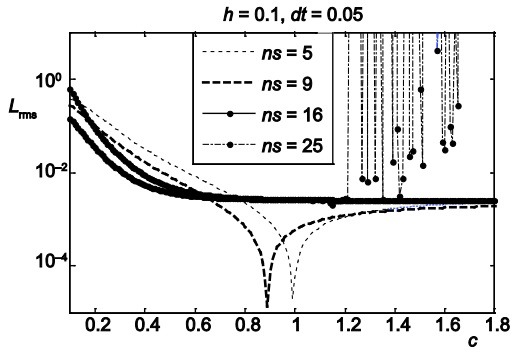


**Figure 2. The evolution curves of $L_{rms}$ with $c$ by using different $ns$**

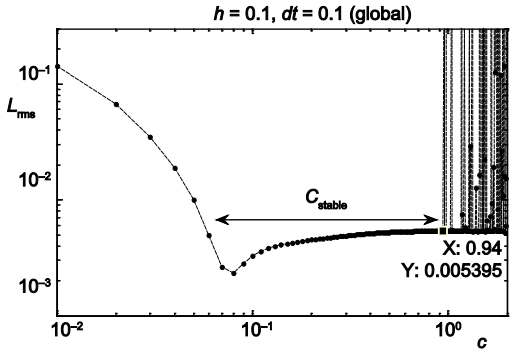


**Figure 3. The $L_{rms}$ error norm by global MQ**

is concluded that the sensitivity of accuracy to $c$ reduces as the value of $ns$ decreases. More precisely, when $ns$ is small (*e. g.*, $ns$ = 5), we can obtain stable results for a large range of $c$. Hence, the selection of $c$ is no longer a problem for local RBF method. Another interesting observation is that if $ns$ is less than 13, there may exist the optimal shape parameter $c$ for some cases. From our experiences, choosing 5 or 9 nodes in the sub-domain will save CPU time and obtain satisfactory numerical results in most cases.

Generally speaking, smaller temporal step and grid distance will lead to higher accuracy for the present numerical approach. But it is also seen that as temporal step gets smaller the range of $C_{stable}$ decreases, which may be partly caused by the memory and hereditary properties of time fractional derivative.

**Table 1. The range of shape parameter and the corresponding root mean squared error upper bound for the Example**

| Nodal model $N$ | Time step $dt$ | 5-point scheme | | 9-point scheme | | 16-point scheme | | 25-point scheme | |
|---|---|---|---|---|---|---|---|---|---|
| | | $L_{rms}$ | $C_{stable}$ | $L_{rms}$ | $C_{stable}$ | $L_{rms}$ | $C_{stable}$ | $L_{rms}$ | $C_{stable}$ |
| 11×11 ($h$ = 0.2) | 0.1 | <8.01E-3 | (2.3, 260) | <2.04E-3 | (2.6, 7.2) | <6.23E-3 | (0.9, 3.3) | <6.72E-3 | (0.8, 2.4) |
| | 0.05 | <5.15E-3 | (3.6, 219) | <5.44E-3 | (1.9, 8.9) | <3.01E-3 | (1.0, 3.3) | <3.99E-3 | (0.8, 2.3) |
| | 0.01 | <2.91E-3 | (4.2, 138) | – | – | <7.46E-4 | (1.1, 3.3) | <1.05E-2 | (1.1, 2) |
| 21×21 ($h$ = 0.1) | 0.1 | <6.74E-3 | (1.6, 159) | <6.50E-3 | (1, 4.7) | <6.63E-3 | (0.6, 2.2) | <6.58E-3 | (0.5, 1.2) |
| | 0.05 | <3.59E-3 | (2.5, 115) | <2.74E-3 | (1.4, 4) | <3.05E-3 | (0.7, 1.8) | <5.32E-3 | (0.4, 1.2) |
| | 0.01 | <1.29E-3 | (3.2, 79) | – | – | <6.99E-4 | (0.8, 1.8) | <9.97E-4 | (0.6, 1.1) |
| 41×41 ($h$ = 0.05) | 0.1 | <5.99E-3 | (0.9, 71) | <5.45E-3 | (0.6, 2) | <6.05E-3 | (0.4, 1.3) | <6.81E-3 | (0.3, 0.6) |
| | 0.05 | <3.44E-3 | (1.3, 73) | <2.59E-3 | (0.85, 1.9) | <2.96E-3 | (0.5, 1.1) | <3.85E-3 | (0.3, 0.6) |
| | 0.01 | <7.48E-4 | (2.4, 35) | – | – | <6.22E-4 | (0.5, 0.9) | – | – |

This paper preliminary studies the application of local RBF method in solving the 2-D time fractional diffusion equations. Further works are still under way, including improving the accuracy of the problems and the optimal $c$ problem.

## Acknowledgments

The work described in this paper was partially supported by Grants from the Research Council of the Hong Kong Special Administrative Region, China (Project No. CityU 101112); the National Basic Research Program of China (973 Project No. 2010CB832702), the National Science Funds for Distinguished Young Scholars (11125208), the R&D Special Fund for Public Welfare Industry (Hydrodynamics, Project No. 201101014) and the National Natural Science Foundation of China under 11202066.

## References

[1] Povstenko, Y. Z., Fractional Heat Conduction Equation and Associated Thermal Stress, *Journal of Thermal Stresses*, *28* (2004), 1, pp. 83-102

[2] Gabano, J. D., Poinot, T., Estimation of Thermal Parameters Using Fractional Modelling, *Signal Processing, 91* (2011), 4, pp. 938-948

[3] Caputo, M., Diffusion of Fluids in Porous Media with Memory, *Geothermics*, 28 (1999), 1, pp. 113-130

[4] Chechkin, A., *et al.*, Fractional Diffusion in Inhomogeneous Media, *Journal of Physics A: Mathematical and General*, *38* (2005), 42, L679

[5] Mainardi, F., Fractional Relaxation-Oscillation and Fractional Diffusion-Wave Phenomena, *Chaos, Solitons & Fractals*, *7* (1996), 9, pp. 1461-1477

[6] Yin, C., *et al.*, Fractional-Order Sliding Mode Based Extremum Seeking Control of a Class of Nonlinear Systems, *Automatica*, *50* (2014), 12, pp. 3173-3181

[7] Li, C., Peng, G., Chaos in Chen's System with a Fractional Order, *Chaos, Solitons & Fractals*, *22* (2004), 2, pp. 443-450

[8] Baleanu, D., *et al.*, Local Fractional Variational Iteration Algorithms for the Parabolic Fokker-Planck Equation Defined on Cantor Sets, *Progr. Fract. Differ. Appl.*, *1* (2014), 1, pp. 1-10

[9] Yang, X.-J., Baleanu, D., Fractal Heat Conduction Problem Solved by Local Fractional Variation Iteration Method, *Thermal Science*, *17* (2013), 2, pp. 625-628

[10] Sun, H. G., *et al.*, A Comparative Study of Constant-Order and Variable-Order Fractional Models in Characterizing Memory Property of Systems, *The European Physical Journal Special Topics*, *193* (2011), 1, pp. 185-192
[11] Bagley, R. L., Torvik, P. J., A Theoretical Basis for the Application of Fractional Calculus to Viscoelasticity, *Journal of Rheology*, *27* (1983), 3, pp. 201-210
[12] Coimbra, C. F. M., Mechanics with Variable-Order Differential Operators, *Annalen der Physik*, *12* (2003), 11-12, pp. 692-703
[13] Chen, W., *et al.*, A Variable-Order Time-Fractional Derivative Model for Chloride Ions Sub-Diffusion in Concrete Structures, *Fractional Calculus and Applied Analysis*, *16* (2013), 1, pp. 76-92
[14] Zhang, Y., *et al.*, Particle Tracking for Time-Fractional Diffusion, *Physical Review E*, *78* (2008), 3, 036705
[15] Tadjeran, C., Meerschaert, M. M., A Second-Order Accurate Numerical Method for the Two-Dimensional Fractional Diffusion Equation, *J. Comput. Phys.*, *220* (2007), 2, pp. 813-823
[16] Murio, D., Implicit Finite Difference Approximation for Time Fractional Diffusion Equations, *Computers & Mathematics with Applications*, *56* (2008), 4, pp. 1138-1145
[17] Sun, H., *et al.*, Finite Difference Schemes for Variable-Order Time Fractional Diffusion Equation, *International Journal of Bifurcation and Chaos*, *22* (2012), 4, pp. 1-16.
[18] Lin, R., *et al.*, Stability and Convergence of a New Explicit Finite-Difference Approximation for the Variable-Order Nonlinear Fractional Diffusion Equation. *Applied Mathematics and Computation*, *212* (2009), 2, pp. 435-445
[19] Chen, C. S., *et al.*, The Method of Approximate Particular Solutions for Solving Certain Partial Differential Equations, *Numerical Methods for Partial Differential Equations*, *28* (2012), 2, pp. 506-522
[20] Liu, Q., *et al.*, An Implicit Rbf Meshless Approach for Time Fractional Diffusion Equations, *Computational Mechanics*, *48* (2011), 1, pp. 1-12
[21] Gu, Y. T., Meshfree Methods and Their Comparisons, *International Journal of Computational Methods*, *2* (2005), 4, pp. 477-515
[22] Chinchapatnam, P. P., *et al.*, Unsymmetric and Symmetric Meshless Schemes for the Unsteady Convection-Diffusion Equation, *Computer Methods in Applied Mechanics and Engineering*, *195* (2006), 19-22, pp. 2432-2453
[23] Fedoseyev, A. I., *et al.*, Improved Multiquadric Method for Elliptic Partial Differential Equations Via Pde Collocation on the Boundary, *Computers & Mathematics with Applications*, *43* (2002), 3-5, pp. 439-455
[24] Uddin, M., On the Selection of a Good Value of Shape Parameter in Solving Time-Dependent Partial Differential Equations Using Rbf Approximation Method, *Applied Mathematical Modelling*, *38* (2014), 1, pp. 135-144
[25] Rippa, S., An Algorithm for Selecting a Good Value for the Parameter C in Radial Basis Function Interpolation, *Advances in Computational Mathematics*, *11* (1999), 2-3, pp. 193-210
[26] Huang, C. S., *et al.*, On the Increasingly Flat Radial Basis Function and Optimal Shape Parameter for the Solution of Elliptic Pdes, *Engineering Analysis with Boundary Elements*, *34* (2010), 9, pp. 802-809
[27] Kansa, E. J., Hon, Y. C., Circumventing the Ill-Conditioning Problem with Multiquadric Radial Basis Functions: Applications to Elliptic Partial Differential Equations, *Computers & Mathematics with Applications*, *39* (2000), 7-8, pp. 123-137
[28] Luh, L.-T., The Mystery of the Shape Parameter IV, *Engineering Analysis with Boundary Elements*, *48* (2014), Nov., pp. 24-31
[29] Yao, G., *et al.*, Assessment of Global and Local Meshless Methods Based on Collocation with Radial Basis Functions for Parabolic Partial Differential Equations in Three Dimensions, *Engineering Analysis with Boundary Elements*, *36* (2012), 11, pp. 1640-1648
[30] Sarler, B., Vertnik, R., Meshfree Explicit Local Radial Basis Function Collocation Method for Diffusion Problems, *Computers & Mathematics with Applications*, 51 (2006), 8, pp. 1269-1282
[31] Hon, Y. C., *et al.*, Local Radial Basis Function Collocation Method for Solving Thermo-Driven Fluid--Flow Problems with Free Surface, *Engineering Analysis with Boundary Elements*, (2015), in press
[32] Divo, E., Kassab, A. J., An Efficient Localized Radial Basis Function Meshless Method for Fluid Flow and Conjugate Heat Transfer, *Journal of Heat Transfer*, *129* (2007), 2, pp. 124-136
[33] Kovacevic, I., Sarler, B., Solution of a Phase-Field Model for Dissolution of Primary Particles in Binary Aluminum Alloys by an R-Adaptive Mesh-Free Method, *Materials Science and Engineering: A*, *413* (2005), Dec., pp. 423-428

[34] Lee, C. K., *et al.*, Local Multiquadric Approximation for Solving Boundary Value Problems, *Computational Mechanics*, *30* (2003), 5-6, pp. 396-409
[35] Yao, G., *et al.*, A Localized Approach for the Method of Approximate Particular Solutions, *Computers & Mathematics with Applications*, *61* (2011), 9, pp. 2376-2387
[36] Hon, Y. C., *et al.*, An Adaptive Greedy Algorithm for Solving Large Rbf Collocation Problems, *Numerical Algorithms*, *32* (2003), 1, pp. 13-25
[37] Sarler, B., *From Global to Local Radial Basis Function Collocation Method for Transport Phenomena*, in *Advances in Meshfree Techniques*, (Eds.: V. M. A. Leitao, C. J. S. Alves, C. Armando Duarte), 2007, Springer, The Netherlands, pp. 257-282
[38] Gao, G.-H., *et al.*, A New Fractional Numerical Differentiation Formula to Approximate the Caputo Fractional Derivative and its Applications, *Journal of Computational Physics*, *259* (2014), Feb., pp. 33-50
[39] Vertnik, R., Sarler, B., Meshless Local Radial Basis Function Collocation Method for Convective-Diffusive Solid-Liquid Phase Change Problems, *International Journal of Numerical Methods for Heat and Fluid Flow*, *16* (2006), 5, pp. 617-640
[40] Sarler, B., A Radial Basis Function Collocation Approach in Computational Fluid Dynamics, *Computer Modelling in Engineering & Sciences*, *7* (2005), 2, pp. 185-193

Paper submitted: October 10, 2014
Paper revised: January 21, 2015
Paper accepted: February 2, 2015